Liquid Crystals
Publication details, including instructions for authors and subscription information:
http://www.informaworld.com/smpp/title~content=t713926090

Exact tilt angle profiles for splay-bend deformations in nematic liquid crystals

C. A. R. Yednak[a]; F. C. M. Freire[a]; E. K. Lenzi[a]; L. R. Evangelista[a]
[a] Departamento de Física, Universidade Estadual de Maringá, Avenida Colombo, 5790-87020-900 Maringá (PR), Brazil

To cite this Article Yednak, C. A. R. , Freire, F. C. M. , Lenzi, E. K. and Evangelista, L. R.(2006) 'Exact tilt angle profiles for splay-bend deformations in nematic liquid crystals', Liquid Crystals, 33: 4, 409 — 415
To link to this Article: DOI: 10.1080/02678290500167931
URL: http://dx.doi.org/10.1080/02678290500167931

Liquid Crystals, Vol. 33, No. 4, April 2006, 409–415

Taylor & Francis
Taylor & Francis Group

Exact tilt angle profiles for splay–bend deformations in nematic liquid crystals

C.A.R. YEDNAK, F.C.M. FREIRE, E.K. LENZI and L.R. EVANGELISTA*

Departamento de Física, Universidade Estadual de Maringá, Avenida Colombo, 5790-87020-900 Maringá (PR), Brazil

(*Received 6 October 2004; in final form 26 April 2005; accepted 26 April 2005*)

The exact tilt angle profiles for splay–bend deformations, in nematic liquid crystal samples limited by inhomogeneous surfaces, are determined in the one-constant approximation. The boundary value problem concerning the situation of strong anchoring at the surfaces of a sample of slab shape of thickness d (Dirichlet's problem) is analytically solved in the presence of an external uniform field. The boundary value problem concerning the weak anchoring situation (mixed problem) is also exactly solved in the absence of an external field. The results are used to obtain the thickness dependence of the optical path difference between the ordinary and extraordinary rays, from which the physical properties of the sample can be deduced.

1. Introduction

Nematic liquid crystals (NLCs) are anisotropic fluids whose physical properties depend on the spatial distribution of the director field **n**. This field gives the local average molecular long axis direction [1]. When the director **n** is parallel everywhere to a plane, as in the case of splay–bend deformation, it may be written in terms of one angle [2]. The evaluation of the director field or of, say, the tilt angle is performed in the framework of the elastic continuum theory [3–6]. In the absence of external fields, the director **n** depends on the surface treatment. According to this treatment it is possible to characterize surface inhomogeneities influencing the NLC orientation. Alignment of the NLC by spatially inhomogeneous surfaces has been analysed following the pioneering work of Berreman [7], who investigated the anchoring effect of a periodically undulating surface where the surface anchoring is locally strong. Since then, the influence of inhomogeneous surfaces on the molecular orientation of an NLC sample has been analysed by several authors in the framework of Frank–Oseen elasticity [8–16]. Some years ago, a complete analytical model for the determination of the profile of the tilt angle was proposed [15] in the strong and weak anchoring hypothesis. The analysis was motivated by the necessity to improve the definition of the surface energy [14] in a continuum description, and the wish to connect the anchoring energy experimentally detected with the random distribution of the easy axes. The same analysis [15] was extended in order to describe walls of orientation induced by sharp variations of the surface treatment [16].

In recent years, the importance of a complete understanding of the alignment of an NLC with patterned isotropic surfaces for practical applications [17] has been recognized. Of particular interest is the investigation of multiple stable NLC orientations for the reduction of power consumption in devices [18]. In these systems, the patterning of a substrate represents a key aspect for the performance of the devices. In general, control of the surface treatment is crucial for the performance of NLC devices and for the understanding of the molecular orientation in NLC samples [19–21].

In this paper, the model proposed in [15] is used to determine the exact profiles of the tilt angle for splay–bend geometry in a sample of NLC in the shape of a slab of thickness d for the cases of strong anchoring (with and without external field) and weak anchoring (without external field) at the treated surfaces. We present, for the first time, the complete analytical solution for the situation of weak anchoring energy, in the one-constant approximation, and using the parabolic approximation for the surface energy, in the absence of electric field. We present also the exact solution of the strong anchoring case in the presence of a uniform external electric field. These exact solutions can be directly employed to establish, in closed forms,

*Corresponding author. Email: lre@dfi.uem.br

Liquid Crystals
ISSN 0267-8292 print/ISSN 1366-5855 online © 2006 Taylor & Francis
http://www.tandf.co.uk/journals
DOI: 10.1080/02678290500167931

the thickness dependence of the optical path difference in real samples.

Our paper is organized as follows. In § 2 the general mathematical formalism for a slab is presented in the general weak anchoring situation. In § 3 the profiles of the tilt angle are explicitly determined for the case of strong anchoring with and without an external electric field. This case corresponds to the mathematical problem known as Dirichlet's problem and is analytically solved in terms of propagators. In § 4 the tilt angle profiles in the situation of weak anchoring (mixed problem) and in the absence of an external electric field is exactly solved. In § 5 the general case in which the anchoring is strong at one of the surfaces and weak at the other, is exactly solved. In § 6 we discuss in detail an application of the previous results, for the case of a periodic distribution of easy axis at the lower surface. The problem is presented for illustrative purposes, due to its connection with the original Berreman problem [7], in order to show how to connect these exact results with the experimentally relevant quantities, such as, the optical path difference. The behaviour of the optical path difference is shown as a function of the ratio between the thickness of the sample and its extrapolation length. Some concluding remarks stressing the applicability of the theoretical tools to relevant experimental situations are presented in § 7.

2. Mathematical problem for a slab

Let us consider a nematic slab of thickness d. The Cartesian reference frame is chosen with the z-axis normal to the bounding plates, located at $z=\pm d/2$. The x-axis is parallel to the direction along which the surface tilt angle is expected to change, and the tilt angle, θ, made by the nematic director with the z-axis, is supposed y-independent and such that $n_x=\sin\theta(x, z)$, $n_y=0$ and $n_x=\cos\theta(x, z)$. In the one-constant approximation, $K_{11}=K_{22}=K_{33}=K$, the bulk free energy density due to elastic distortions is given by [1]

$$f_{\mathrm{b}}=\frac{1}{2}K\left(\vec{\nabla}\theta\right)^2 \tag{1}$$

where $\vec{\nabla}\theta=\mathbf{i}(\partial\theta/\partial x)+\mathbf{k}(\partial\theta/\partial z)$, whilst $\mathbf{i}$ and $\mathbf{k}$ are the unit vectors parallel to the x-and z-axes, respectively. The general situation can be analysed by taking into account the existence of a finite surface energy which we will assume to be of the kind proposed by Rapini and Papoular [22], but in the parabolic approximation, i.e. $f_s=(W/2)(\theta-\Theta)^2$, where W is the anchoring strength. This approximation implies that we are considering only deformations for which the difference between the actual tilt angle at the surface and the easy direction imposed by the surface is small. The strong anchoring case corresponds to the limit $W\to\infty$. The total elastic free energy of the nematic sample, per unit length along the y-axis, is given by

$$F[\theta(x, z)]=\int_{-\infty}^{\infty}\mathrm{d}x\int_{-d/2}^{d/2}\mathrm{d}z\frac{1}{2}K\left(\vec{\nabla}\theta\right)^2 + \int_{-\infty}^{\infty}\frac{1}{2}\left\{\begin{array}{l} W_-\,[\theta_-(x)-\Theta_-(x)]^2 \\ +W_-\,[\theta_+(x)-\Theta_+(x)]^2\end{array}\right\}\mathrm{d}x \tag{2}$$

where $\theta_\pm(x)$ is the actual value of the surface tilt angle, W_- and W_+ refer to the low and upper surface respectively. Hereafter, for simplicity, we will assume that $W_-=W_+=W$. The principle of the continuum theory states that the actual director profile, or $\theta(x, z)$, is deduced by minimizing the total free energy given by equation (2). Usual calculations give

$$\frac{\partial^2\theta}{\partial x^2}+\frac{\partial^2\theta}{\partial z^2}=0,\quad -\infty<x<\infty,\quad -\frac{d}{2}\le z\le\frac{d}{2}. \tag{3}$$

The solution is a harmonic function $\theta(x, z)$ which needs to satisfy appropriate boundary conditions. In the general case of weak anchoring the boundary conditions are [23]:

$$\pm L\left[\frac{\partial\theta}{\partial z}\right]_{z=\pm d/2}+\theta_\pm(x)-\Theta_\pm(x)=0. \tag{4}$$

In equation (4), $L=K/W$ is the extrapolation length [8], and $\Theta_\pm(x)$ accounts for the surface orientation imposed by the surface treatment, i.e. the easy axes on the upper and lower surfaces, respectively. It is possible to show that the general solution of equation (3), satisfying boundary conditions (4), can be expressed in terms of propagators as [15, 16]

$$\theta_W(x, z)=\int_{-\infty}^{\infty}\left[\begin{array}{l} G_+(x'-x, z)\theta_+(x') \\ +G_-(x'-x, z)\theta_-(x')\end{array}\right]\mathrm{d}x' \tag{5}$$

where

$$G_\pm(x'-x, z)=\frac{1}{2d}\frac{\cos(\pi z/d)}{\cosh[\pi(x'-x)/d]\mp\sin(\pi z/d)}. \tag{6}$$

By substituting the general solution into the boundary conditions equation (4), one obtains

$$\theta_\pm=\Theta_\pm\pm L\int_{-\infty}^{\infty}\mathrm{d}x'\left[\begin{array}{l}\theta_+(x)h_+(x-x', z) \\ +\theta_-(x)h_-(x-x', z)\end{array}\right]_{z=\pm d/2} \tag{7}$$

where $h_\pm(x-x', z)=\partial G_\pm(x-x', z)/\partial z$. Therefore, to solve the boundary value problem relative to the weak anchoring situation, one has to solve the set of two coupled Fredholm integral equations of second kind in equations (7) in order to obtain the tilt angle at the surfaces $\theta_{\pm}$. Once a solution is obtained, equation (5) can be used to give the tilt angle profile. In the next section we present an alternative way to solve the problem.

3. Strong anchoring case

3.1. *No external field*

Let us first consider the simple case of strong anchoring, which corresponds to the limit $L \to 0$. In this case, equation (4) reduces to

$$\theta\left(x, \pm\frac{d}{2}\right) = \Theta_{\pm}(x) \tag{8}$$

and the exact solution is simply written as

$$\theta_S(x, z) = \int_{-\infty}^{\infty} \sum\nolimits_i G_i(x' - x, z)\Theta_i(x')\mathrm{d}x' \tag{9}$$

where i=+, −. Equations (6) and (9) give the complete solution of the problem in the strong anchoring hypothesis and has been discussed in detail in [15, 16].

3.2. *External uniform electric field*

When the NLC is submitted to an electric field, **E**, parallel to z, the total energy per unit length along y may be written as

$$F[\theta(x, z)] = \int_{-\infty}^{\infty} \mathrm{d}x \int_{-d/2}^{d/2} \mathrm{d}z \left[\frac{1}{2}K\left(\vec{\nabla}\theta\right)^2 + \frac{\varepsilon_a}{2}E^2\theta^2\right] + \int_{-\infty}^{\infty} \frac{1}{2}\left\{\begin{array}{l} W_-[\theta_-(x) - \Theta_-(x)]^2 \\ + W_-[\theta_+(x) - \Theta_+(x)]^2 \end{array}\right\}\mathrm{d}x \tag{10}$$

in the limit of small θ. In equation (10) $\varepsilon_a = \varepsilon_{\|} - \varepsilon_{\perp}$ (‖ and ⊥ refer to the direction of **n**) is the dielectric anisotropy. By minimizing (10) we obtain

$$\frac{\partial^2\theta}{\partial x^2} + \frac{\partial^2\theta}{\partial z^2} = \alpha^2\theta \tag{11}$$

where $\alpha^2 = (\varepsilon_a/K)E^2$. In order to obtain the solution for this equation, we start by considering the Fourier transform of equation (11) on the x variable, which yields:

$$-k^2\theta(k, z) + \frac{\mathrm{d}^2}{\mathrm{d}z^2}\theta(k, z) = \alpha^2\theta(k, z). \tag{12}$$

By solving the above equation, we obtain in the k-space the solution

$$\theta(k, z) = G_+(k, z)\Theta_+(k) + G_-(k, z)\Theta_-(k) \tag{13}$$

with

$$G_{\pm}(k, z) = \frac{\sinh\left[\left(k^2 + \alpha^2\right)^{\frac{1}{2}}(d/2 \pm z)\right]}{\sinh\left[\left(k^2 + \alpha^2\right)^{\frac{1}{2}}d\right]}. \tag{14}$$

Now, by using the inverse Fourier transform, and taking the convolution theorem into account, we obtain

$$\theta(x, z) = \int_{-\infty}^{\infty} \sum_i G_i(x - x', z)\Theta_i(x')\mathrm{d}x' \tag{15}$$

where, as before, i=+, − and

$$G_{\pm}(x, z) = \sum_{n=1}^{\infty} \begin{array}{c} (-1)^{n+1}\dfrac{n\pi\sin[n\pi/d(d/2 \pm z)]}{d\left[(n\pi)^2 + (\alpha d)^2\right]^{\frac{1}{2}}} \\ \exp\left\{-\left[(n\pi/d)^2 + \alpha^2\right]^{\frac{1}{2}}|x|\right\} \end{array} \tag{16}$$

Note that by removing the electric field, **E**, from the above equation, i.e. by putting $\alpha = 0$, we recover the result obtained in equation (6) for the strong anchoring case in the absence of an external field.

4. Weak anchoring situation: mixed problem

To face the mixed boundary - value problem, in the absence of an external electric field, instead of solving the system of two coupled integral equations represented by equation (7), we start again by considering the Fourier transform of equation (3), which yields:

$$\frac{\mathrm{d}^2\vartheta(k, z)}{\mathrm{d}z^2} - k^2\vartheta(k, z) = 0 \tag{17}$$

where

$$\vartheta(k, z) = \int_{-\infty}^{\infty} \mathrm{d}x\, \exp(-\mathrm{i}kx)\theta(x, z). \tag{18}$$

A particular solution of equation (17) may be written as

$$\vartheta(k, z) = \mathcal{C}_1(k)\exp(kz) + \mathcal{C}_2(k)\exp(-kz). \tag{19}$$

In the same manner, by Fourier transforming the boundary conditions, equation (4), we obtain

$$\pm L\left[\frac{\mathrm{d}\vartheta}{\mathrm{d}z}\right]_{z=\pm d/2} + \vartheta_{\pm}(k) - \Phi_{\pm}(k) = 0, \tag{20}$$

with $\vartheta_{\pm}(k) = \vartheta(k, \pm d/2)$ and

$$\Phi_{\pm}(k) = \int_{-\infty}^{\infty} \mathrm{d}x\, \exp(-\mathrm{i}kx)\Theta_{\pm}(x). \tag{21}$$

By substituting equation (19) into (20) one easily obtains the system of equations

$$\begin{aligned}(1+kL)e^{kd/2}\mathcal{C}_1(k)+(1-kL)e^{-kd/2}\mathcal{C}_2(k)&=\Phi_+(k)\\(1-kL)e^{-kd/2}\mathcal{C}_1(k)+(1+kL)e^{kd/2}\mathcal{C}_2(k)&=\Phi_-(k),\end{aligned}\tag{22}$$

giving

$$\begin{aligned}\mathcal{C}_1(k)&=\frac{(1+kL)\exp(kd/2)\Phi_+(k)-(1-kL)\exp(-kd/2)\Phi_-(k)}{(1+kL)^2\exp(kd)-(1-kL)^2\exp(-kd)}\\\mathcal{C}_2(k)&=\frac{(1+kL)\exp(kd/2)\Phi_-(k)-(1-kL)\exp(-kd/2)\Phi_+(k)}{(1+kL)^2\exp(kd)-(1-kL)^2\exp(-kd)}.\end{aligned}\tag{23}$$

To proceed further, we note that, after some manipulations of equations (19) and (23), $\vartheta(k, z)$ can be written as

$$\vartheta(k,z)=\mathcal{G}_+(k,z)\Phi_+(k)+\mathcal{G}_-(k,z)\Phi_-(k)\tag{24}$$

where

$$\mathcal{G}_\pm(k,z)=\frac{\sinh[k(d/2\pm z)]+kL\cosh[k(d/2\pm z)]}{\left[1+(kL)^2\right]\sinh(kd)+2kL\cosh(kd)}.\tag{25}$$

In this way, the problem is formally solved in the k-space. To obtain $\theta(x, z)$, we have to consider the inverse Fourier transform of equation (25) and the convolution theorem, namely

$$\begin{aligned}\theta(x,z)&=\mathcal{F}^{-1}\{\mathcal{G}_+(k,z)\Phi_+(k)\}+\mathcal{F}^{-1}\{\mathcal{G}_-(k,z)\Phi_-(k)\}\\&=\int_{-\infty}^{\infty}\mathrm{d}x'\sum_i\mathcal{G}_i(x-x',z)\Theta_i(x')\end{aligned}\tag{26}$$

with $i=-, +$ and

$$\mathcal{G}_\pm(x,z)=\int_{-\infty}^{\infty}\frac{\mathrm{d}k}{2\pi}\exp(\mathrm{i}kx)\mathcal{G}_\pm(k,z).\tag{27}$$

Explicit formulae for the new propagator can be obtained by performing the above integration with the help of the method of residues [24]. One obtains

$$\mathcal{G}_\pm(x,z)=\sum_{n=1}^{\infty}\frac{\sin[k_n(d/2\pm z)]+k_nL\cos[k_n(d/2\pm z)]}{2k_nL(L+d)\sin(k_nd)-\left[\left(1-(k_nL)^2\right)d+2L\right]\cos(k_nd)}\exp(-k_n|x|)\tag{28}$$

with $k_n>0$. The values of k_n are obtained from equation $2k_nL\cos(k_nd)+[1-(k_nL)^2]\sin(k_nd)=0$. Equation (28) is an extension from (6) by considering an extrapolation length and it also recovers equation (6) for $L\to 0$.

5. Combined situations of weak and strong anchoring

Let us consider now the case in which at one of the surfaces the situation is of strong anchoring, and at the other the anchoring is weak. Specifically, consider that

$$\begin{aligned}\theta\left(x,\frac{d}{2}\right)&=\Theta_+(x)\\-L\left[\frac{\partial\theta}{\partial z}\right]_{z=-d/2}+\theta_-(x)-\Theta_-(x)&=0.\end{aligned}\tag{29}$$

By using the Fourier transform, we can reduce equation (3) to

$$-k^2\theta(k,z)+\frac{\mathrm{d}^2}{\mathrm{d}z^2}\theta(k,z)=0.\tag{30}$$

The solution for the above equation in the k-space is

$$\theta(k,z)=\mathcal{C}_1'(k)\exp(kz)+\mathcal{C}_2'(k)\exp(-kz)\tag{31}$$

Now applying the boundary conditions, we obtain

$$\begin{aligned}\exp(kd/2)\mathcal{C}_1'(k)+\exp(-kd/2)\mathcal{C}_2'(k)&=\Theta_+(k)\\(1-kL)\exp(-kd/2)\mathcal{C}_1'(k)&\\+(1+kL)\exp(kd/2)\mathcal{C}_2'(k)&=\Theta_-(k).\end{aligned}\tag{32}$$

From the above set of equations we easily obtain $\mathcal{C}_1'(k)$ and $\mathcal{C}_2'(k)$. Therefore, equation (31) can be rewritten as

$$\theta(k,z)=\mathcal{G}_+'(k,z)\Theta_+(k)+\mathcal{G}_-'(k,z)\Theta_-(k)\tag{33}$$

which, by using the inverse of Fourier transform is reduced to

$$\theta(x,z)=\int_{-\infty}^{\infty}\mathrm{d}x'\sum_i\mathcal{G}_i'(x-x',z)\Theta_i(x')\tag{34}$$

where, again, $i=-, +$ and

$$\begin{aligned}\mathcal{G}_+(x,z)&=\sum_{n=1}^{\infty}\frac{\sin\left[\bar{k}_n(d/2+z)\right]+\bar{k}_nL\cos\left[\bar{k}_n(d/2+z)\right]}{\bar{k}_nLd\sin\left(\bar{k}_nd\right)-(d+L)\cos\left(\bar{k}_nd\right)}\exp\left(-\bar{k}_n|x|\right)\\\mathcal{G}_-(x,z)&=\sum_{n=1}^{\infty}\frac{\sin\left[\bar{k}_n(d/2-z)\right]}{\bar{k}_nLd\sin\left(\bar{k}_nd\right)-(d+L)\cos\left(\bar{k}_nd\right)}\exp\left(-\bar{k}_n|x|\right)\end{aligned}\tag{35}$$

with $\bar{k}_n>0$. The values of $\bar{k}_n$ are obtained from the equation $\bar{k}_nL\cos\left(\bar{k}_nd\right)+\sin\left(\bar{k}_nd\right)=0$.

6. Illustrative examples

In order to explore the generality of the solution represented by equation (9), we first consider, for illustrative purposes, a problem dealing with a periodic distribution of easy axes [14]. We consider a sample in the shape of a slab as in figure 1, such that

$$\Theta_+(x)=\Theta_0,\quad\text{and}\quad\Theta_-(x)=\begin{cases}\Theta_1, & 0<x<a\\\Theta_2, & a<x<2a\end{cases}\tag{36}$$

indicating that the easy axes at the lower surface is distributed with a periodicity $\lambda=2a$. In general terms,

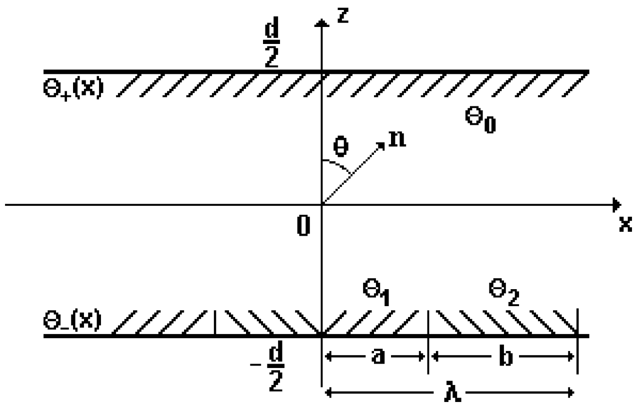

Figure 1. Nematic sample of thickness d whose upper surface, located at $z=d/2$, is characterized by a uniform orientation Θ_0, whereas the lower surface is characterized by a periodic distribution of easy axes, such that $\lambda=2a$ ($b=a$).

the boundary conditions may be rewritten as

$$\begin{aligned}&\Theta_+(x)=\Theta_0 \quad \text{and}\\ &\Theta_-(x)=\Theta_1+(\Theta_2-\Theta_1)\\ &\sum_{n=0}^{\infty}(-1)^n[\mathrm{H}(x-na)+\mathrm{H}(-x-(n+1)a)]\end{aligned} \tag{37}$$

where $H(x)$ is the Heaviside step function.

6.1. *Strong anchoring case*

In the strong anchoring situation we have to solve the Dirichlet problem, i.e. to find a solution for equation (3) satisfying boundary conditions (8), when $\Theta_\pm$ is distributed according to equation (37). In this case the general solution of the problem may be written as

$$\begin{aligned}\theta(x,z)=&\Theta_0\Delta_+ + \Theta_1\Delta_-\\ &+(\Theta_2-\Theta_1)\sum_{n=0}^{\infty}(-1)^n\left\{\arctan\left[\frac{\cos\left(\frac{\pi z}{2d}\right)-\sin\left(\frac{\pi z}{2d}\right)}{\cos\left(\frac{\pi z}{2d}\right)+\sin\left(\frac{\pi z}{2d}\right)}\tanh\left[\frac{\pi}{2d}(x-na)\right]\right]\right.\\ &\left.-\arctan\left[\frac{\cos\left(\frac{\pi z}{2d}\right)-\sin\left(\frac{\pi z}{2d}\right)}{\cos\left(\frac{\pi z}{2d}\right)+\sin\left(\frac{\pi z}{2d}\right)}\tanh\left[\frac{\pi}{2d}(x+(1+n)a)\right]\right]+2\Delta_-\right\}\end{aligned} \tag{38}$$

where, to save space, we have introduced the quantities:

$$\Delta_\pm=\frac{2}{\pi}\arctan\left[\frac{\cos\left(\frac{\pi z}{2d}\right)\pm\sin\left(\frac{\pi z}{2d}\right)}{\cos\left(\frac{\pi z}{2d}\right)\mp\sin\left(\frac{\pi z}{2d}\right)}\right]. \tag{39}$$

6.2. *Weak anchoring case*

In the weak anchoring situation, we again have to solve equation (3), but now subjected to the boundary conditions (4), when the easy axes are given by equation (37). After some algebra, a closed solution is obtained, namely

$$\begin{aligned}\theta(x,z)=&2\Theta_0\sum_{n=1}^{\infty}\frac{f_+(k_n,z)}{k_n}+2\Theta_1\sum_{n=1}^{\infty}\frac{f_-(k_n,z)}{k_n}+(\Theta_2-\Theta_1)\\ &\times\sum_{n=1}^{\infty}\frac{f_-(k_n,z)}{k_n}\sum_{m=0}^{\infty}(-1)^m\{[2-\exp[-k_n(x-ma)]]H(x-ma)\\ &+\exp[-k_n(ma-x)]H(ma-x)+\exp[-k_n(x+(m+1)a)]H(x+(m+1)a)\\ &+[2-\exp[k_n(x+(m+1)a)]]H(-x-(m+1)a)\}\end{aligned} \tag{40}$$

where

$$f_\pm(k_n,z)=\frac{\sin[k_n(d/2\pm z)]+k_nL\cos[k_n(d/2\pm z)]}{2k_nL(L+d)\sin(k_nd)-\left[\left(1-(k_nL)^2\right)d+2L\right]\cos(k_nd)}. \tag{41}$$

As a final illustration, we can consider the following distribution of easy axis

$$\Theta_+(x)=\Theta_0, \quad \text{and} \quad \Theta_-(x)=\Theta_1\sin(qx) \tag{42}$$

in which $q=2\pi/\lambda$, where λ is connected with the spatial periodicity of the sinusoidal distribution of the easy axis. The general case refers to the weak anchoring situation, i.e. the problem is solved for the boundary conditions (4). One easily obtains for the profile of the tilt angle:

$$\theta(x,z)=2\Theta_0\sum_{n=1}^{\infty}\frac{f_+(k_n,z)}{k_n}+2\Theta_1\sum_{n=1}^{\infty}\frac{f_-(k_n,z)}{q^2+k_n^2}k_n\sin(qx) \tag{43}$$

with $f_\pm(k_n, z)$ given by equation (41). The above solutions show that a very large class of problems may be exactly solved with the formalism we have presented.

When $\theta(x, z)$ is known, the physical properties of the NLC sample can be explored. For example, in the case in which a linear polarized beam impinges normally on the nematic sample, the optical path difference Δl [25], between the ordinary and the extraordinary ray is

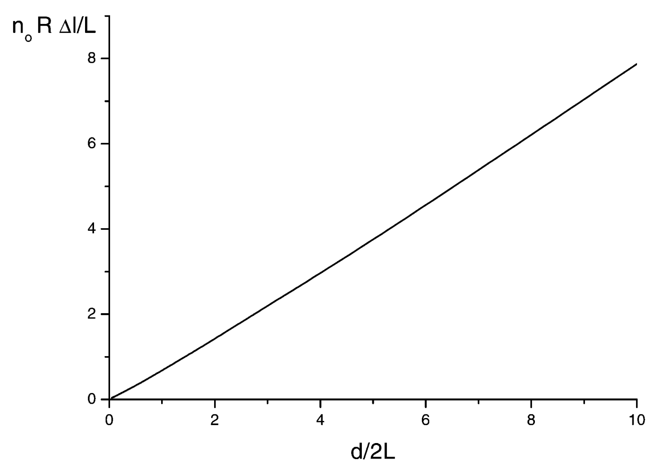

Figure 2. Optical path difference $n_oR\Delta l/L$ vs reduced thickness $d/2L$, for $\lambda=L$, $\Lambda/2L=5$, $\Theta_0=\pi/4$, and $\Theta_1=\pi/2$.

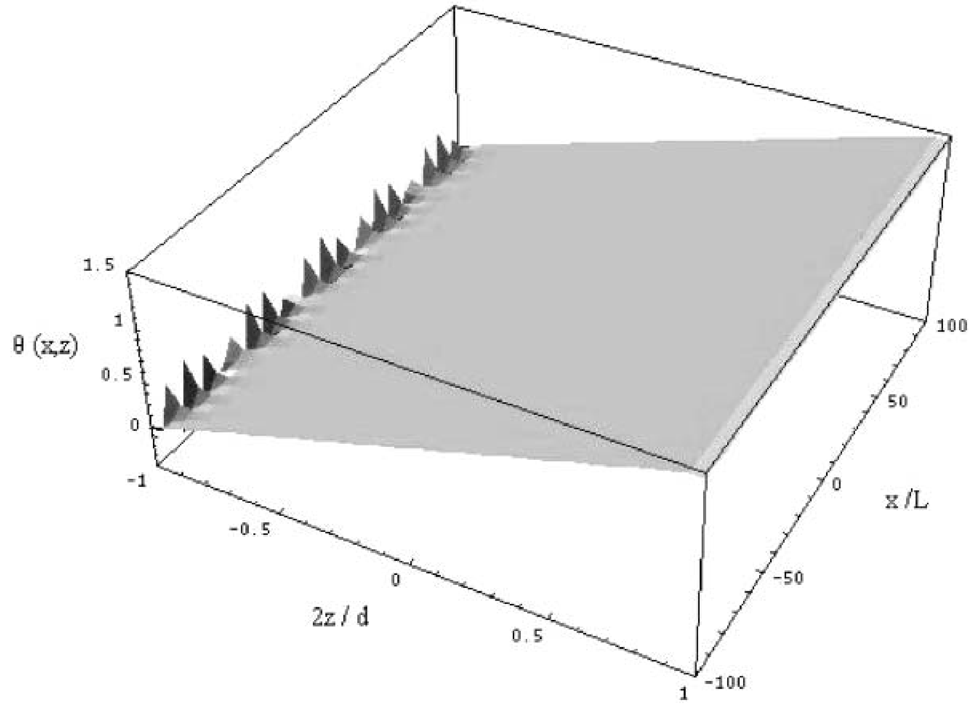

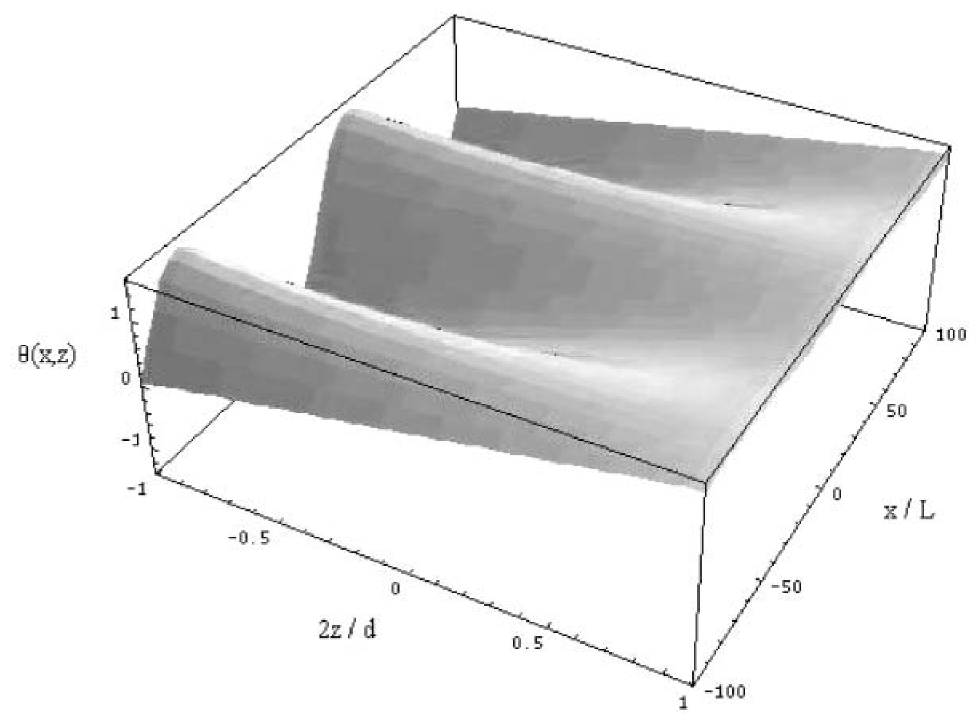

Figure 3. Tilt angle profile $\theta(x, z)$ vs reduced coordinates $2z/d$ and x/L for $\lambda=L$ (upper) and $\lambda=100L$ (lower). Both surfaces are characterized by weak anchoring and the curves have been depicted for $d/2L=10$, $\Lambda/2L=100$, and $\Theta_0=\Theta_1=\pi/2$.

given by

$$\Delta l=\frac{1}{\Lambda}\int_{-\Lambda/2}^{\Lambda/2}\int_{-d/2}^{d/2}\Delta n(\theta)\mathrm{d}x\,\mathrm{d}z=\frac{1}{2}n_o R d\langle\theta^2\rangle \qquad (44)$$

where

$$\langle\theta^2\rangle=\frac{1}{d\Lambda}\int_{-\Lambda/2}^{\Lambda/2}\int_{-d/2}^{d/2}\theta(x,z)^2\mathrm{d}x\,\mathrm{d}z \qquad (45)$$

is the average square tilt angle, evaluated over a typical length Λ, connected with the diameter of the light beam. Furthermore, $R=1-(n_o/n_e)^2$, and n_o and n_e are, respectively, the ordinary and extraordinary refractive indices. In figure 2 the optical path difference is shown as a function of the reduced thickness $d/2L$ for a nematic medium whose distribution of easy axes at the surfaces is given by equation (42). Due to the different easy axes on both surfaces, the sample is distorted for any finite thickness, i.e. $\Delta l \neq 0$ for every d. As expected, $\Delta l \to 0$ when $d \to 0$. The distortions are illustrated in figure 3 for two different values of $\lambda=2p/q$. In the upper part of figure 3, $\lambda=L$ and the distortions in the director profile are strongly localized near the lower surface, at $2z/d=-1$, for which the easy axis distribution is periodic. The tilt angle profile is practically uniform for the rest of the sample. In the lower part of figure 3, $\theta(x, z)$ is shown for $\lambda=100L$. In this case, the entire sample is distorted. Near the upper surface the orientation tends to become more uniform: θ tends to a constant value less than $\Theta_0=\pi/2$, because the anchoring is weak at that surface. Note that we are working in the approximation for which the difference between the actual tilt angle and the angle characterizing the easy direction is small. Therefore, we only require the relative difference between θ and Θ_0 (or Θ_1) to be small, which is the case illustrated in figure 3.

7. Concluding remarks

Exact tilt angle profiles have been determined for a nematic liquid crystal sample of thickness d, when only splay–bend deformations are allowed in the system. Different situations of surface inhomogeneities have been considered in the case of strong and weak anchoring at the surfaces, in the one-constant approximation. Boundary-value problems connected with the Laplace equation in two dimensions (representing the situation of the absence of an external field) have been solved in closed analytical form. The tilt angle profile for the case of weak anchoring, representing the mixed boundary-value problem, has been exactly obtained for a large class of representative distributions of the easy axes at the surfaces. The Dirichlet's problem (strong anchoring case) was solved for a sample submitted to an external uniform electric field. The general results have been applied to a few illustrative cases. In particular, the case in which at one of the surfaces the easy axis distribution is periodic, whereas at the other it is uniform (in the case of weak anchoring) is discussed. For this representative case, the optical path difference was calculated as a function of the reduced thickness of the sample ($d/2L$), indicating that the molecular orientation is never uniform, even for arbitrary values of thickness. The tilt angle profiles are shown to be strongly dependent of the value of the spatial periodicity λ of the distribution of the easy axis. For small values of $\lambda(\lambda \approx L)$ the deformations are localized near the surface, whereas for $\lambda > L$, the distortions extend over the entire sample.

Acknowledgements

Many thanks are due to G. Barbero (Torino) for useful discussions. This work was supported by Brazilian Agencies Capes, CNPq, and Fundação Araucária.

References

[1] P.G. de Gennes. *The Physics of Liquid Crystals*, Clarendon Press, Oxford (1974).
[2] S. Chandrasekhar. *Liquid Crystals*, Cambridge Univeristy Press, Cambridge (1977).
[3] C.W. Oseen. *Trans. Faraday. Soc.*, **29**, 883 (1933).
[4] F.C. Frank. *Discuss. Faraday. Soc.*, **25**, 19 (1958).
[5] J.L. Ericksen. *Adv. Liq. Cryst.*, **2**, 233 (1976).
[6] F.M. Leslie. In *Theory and Applications of Liquid Crystals*, J.L. Ericksen, D. Kinder Leher (Eds), Springer-Verlag, Berlin (1987).
[7] W. Berreman. *Phys. Rev. Lett.*, **28**, 1683 (1972).
[8] M. Kléman. *Points, Lignes, Parois*, Editions de Physique, Les Ulis, Orsay (1977).
[9] G. Barbero. *Lett. nuovo Cimento*, **29**, 553 (1980).
[10] G. Barbero. *Lett. nuovo Cimento*, **32**, 60 (1981).
[11] H.L. Ong, A.J. Hurd, R.B. Meyer. *J. appl. Phys.*, **57**, 186 (1985).
[12] F. Lonberg, R.B. Meyer. *Phys. Rev. Lett.*, **55**, 718 (1985).
[13] S. Faetti. *Phys. Rev. A*, **36**, 408 (1987).
[14] G. Barbero, T. Beica, A.L. Alexe-Ionescu, R. Moldovan. *J. Phys. (Paris) II*, **2**, 2011 (1992).
[15] L.R. Evangelista, G. Barbero. *Phys. Rev. E*, **48**, 1163 (1993).
[16] L.R. Evangelista, G. Barbero. *Phys. Rev. E*, **50**, 2120 (1994).
[17] B. Lee, N. Clark. *Science*, **291**, 2576 (2001).
[18] J.H. Kim, M. Yoneya, H. Yokoyama. *Nature*, **420**, 159 (2002).
[19] T.Z. Qian, P. Sheng. *Phys. Rev. E*, **55**, 7111 (1997).
[20] B. Zhang, F. Lee, O.K.C. Tsui, P. Sheng. *Phys. Rev. Lett.*, **91**, 215501 (2003).
[21] O.K.C. Tsui, F.K. Lee, B. Zhang, P. Sheng. *Phys. Rev. E*, **69**, 021704 (2004).
[22] A. Rapini, M. Papoular. *J. Phys. (Paris) Colloq.*, **30**, C4–54 (1969).
[23] G. Barbero, L.R. Evangelista. *An Elementary Course on the Continuum Theory for Nematic Liquid Crystals*, World Scientific, Singapore (2001).
[24] P.M. Morse, H. Feshbach. In *Methods of Theoretical Physics* Vol. I, Chap. 8, McGraw-Hill, New York (1953).
[25] G. Barbero, R. Barberi. In *The Physics of Liquid Crystalline Materials*, I.C. Khoo, F. Simoni (Eds), Gordon and Breach (1988).